

$B^* \rightarrow \bar{D}D$ decays with perturbative QCD approach

Junfeng Sun,¹ Haiyan Li,¹ Yueling Yang,¹ Na Wang,¹ Qin Chang,¹ and Gongru Lu¹

¹*Institute of Particle and Nuclear Physics,
Henan Normal University, Xinxiang 453007, China*

Abstract

The nonleptonic two-body $B^* \rightarrow \bar{D}D$ weak decays are studied phenomenologically with the perturbative QCD factorization approach. It is found that the $B_s^{*0} \rightarrow D_s^- D_s^+$, $B_d^{*0} \rightarrow D_d^- D_s^+$, and $B_u^{*+} \rightarrow \bar{D}_u^0 D_s^+$ decays have branching ratios $\gtrsim 10^{-9}$, and might be promisingly measurable at the running LHC and forthcoming SuperKEKB experiments in the future.

I. INTRODUCTION

The B_q^* mesons, consisting of $\bar{b}q$ pair with $q = u, d$ and s , are spin-triplet ground vector states with definite spin-parity quantum numbers of $J^P = 1^-$ [1]. Because the mass splittings $m_{B_q^*} - m_{B_q} \lesssim 50$ MeV [1] are much smaller than the mass of the lightest pion meson, the B_q^* meson decays dominantly into the ground pseudoscalar B_q meson through the electromagnetic interaction. Besides, the B_q^* mesons can also decay via the bottom-changing transition induced by the weak interaction within the standard model (SM). Because of the strong phase-space suppression from their dominant magnetic dipole (M1) transition $B_q^* \rightarrow B_q \gamma$, the lifetime of the B_q^* meson is of the order of 10^{-17} second or less, which, in general, is too short to enable the B_q^* meson to experience the weak disintegration [2]. The B_q^* weak decays have not actually attracted much attention yet. Until now, there has been no experimental report and few theoretical works concentrating on the B_q^* weak decay, subject to the relatively inadequate statistics on the B_q^* mesons. Fortunately, the high luminosities and large production rates at LHC and the forthcoming SuperKEKB are promising, and the rapid accumulation of more and more B_q^* data samples is expected to be possible. Some B_q^* weak decay modes might be detected and investigated in the future, which undoubtedly makes the B_q^* mesons another a vibrant arena for testing the Cabibbo-Kabayashi-Maskawa (CKM) picture for CP -violating phenomena, examining our comprehension of the underlying dynamical factorization mechanism, and so on. In addition, heavy quark symmetry relates hadronic transition matrix elements (HTME) of the B_q^* and B_q weak decays. The interplay between the B_q^* and B_q weak decays could prove useful information to overconstrain parameters in the SM, and might shed some fresh light on various anomalies in B decays.

The purely leptonic decays $B_q^* \rightarrow \ell^+ \ell^-$ induced by the flavor-changing neutral currents have been studied recently in the SM [2, 3]. The semileptonic and nonleptonic B_q^* decays have been investigated also in the SM [4–7], where the transition form factors are evaluated with the Wirbel-Stech-Bauer approach [8], and the nonfactorizable corrections to HTME are considered [5, 6] based on the collinear-based and QCD-improved factorization (QCDF) approach [9–13]. In this paper, we will study the nonleptonic B_q^* decay into the pseudoscalar charmed-meson pair $\bar{D}D$ with the perturbative QCD factorization (pQCD) approach [14–16], just to provide a ready reference for the future experimental research. In addition, as

is well known, the production ratio for the B_q^* meson is comparable with that for the B_q meson (see Table III), the B_q^* and B_q mesons have nearly equal mass. Hence, the study of the $B_q^* \rightarrow \overline{D}D$ decays will undoubtedly be helpful to the experimental background analysis on the $B_q \rightarrow \overline{D}D$ decays.

This paper is organized as follows. The theoretical framework and amplitudes for $B_q^* \rightarrow \overline{D}D$ decays with pQCD approach are given in section II. Section III is devoted to numerical results and discussion. The final section is a summary.

II. THEORETICAL FRAMEWORK

A. The effective Hamiltonian

The effective Hamiltonian describing the $B_q^* \rightarrow \overline{D}D$ weak decay is written as [17]

$$\mathcal{H}_{\text{eff}} = \frac{G_F}{\sqrt{2}} \sum_{q=d,s} \left\{ \sum_{p=u,c} V_{pb}^* V_{pq} \sum_{i=1}^2 C_i(\mu) Q_i(\mu) - V_{tb}^* V_{tq} \sum_{k=3}^{10} C_k(\mu) Q_k(\mu) \right\} + \text{h.c.}, \quad (1)$$

where the Fermi coupling constant $G_F \simeq 1.166 \times 10^{-5} \text{ GeV}^{-2}$ [1]; $V_{pb}^* V_{pq}$ and $V_{tb}^* V_{tq}$ are the CKM factors; The scale μ factorizes the physical contributions into two parts: the Wilson coefficients C_i and the local four-fermion operators Q_i . The operators are defined as follows.

$$Q_1 = (\bar{b}_\alpha p_\alpha)_{V-A} (\bar{p}_\beta q_\beta)_{V-A}, \quad Q_2 = (\bar{b}_\alpha p_\beta)_{V-A} (\bar{p}_\beta q_\alpha)_{V-A}, \quad (2)$$

$$Q_3 = \sum_{q'} (\bar{b}_\alpha q_\alpha)_{V-A} (\bar{q}'_\beta q'_\beta)_{V-A}, \quad Q_4 = \sum_{q'} (\bar{b}_\alpha q_\beta)_{V-A} (\bar{q}'_\beta q'_\alpha)_{V-A}, \quad (3)$$

$$Q_5 = \sum_{q'} (\bar{b}_\alpha q_\alpha)_{V-A} (\bar{q}'_\beta q'_\beta)_{V+A}, \quad Q_6 = \sum_{q'} (\bar{b}_\alpha q_\beta)_{V-A} (\bar{q}'_\beta q'_\alpha)_{V+A}, \quad (4)$$

$$Q_7 = \sum_{q'} \frac{3}{2} Q_{q'} (\bar{b}_\alpha q_\alpha)_{V-A} (\bar{q}'_\beta q'_\beta)_{V+A}, \quad Q_8 = \sum_{q'} \frac{3}{2} Q_{q'} (\bar{b}_\alpha q_\beta)_{V-A} (\bar{q}'_\beta q'_\alpha)_{V+A}, \quad (5)$$

$$Q_9 = \sum_{q'} \frac{3}{2} Q_{q'} (\bar{b}_\alpha q_\alpha)_{V-A} (\bar{q}'_\beta q'_\beta)_{V-A}, \quad Q_{10} = \sum_{q'} \frac{3}{2} Q_{q'} (\bar{b}_\alpha q_\beta)_{V-A} (\bar{q}'_\beta q'_\alpha)_{V-A}, \quad (6)$$

where $Q_{1,2}$ are tree operators arising from the W -boson exchange; $Q_{3,\dots,6}$ and $Q_{7,\dots,10}$ are called the QCD and electroweak penguin operators, respectively; $(\bar{q}_1 q_2)_{V\pm A} \equiv \bar{q}_1 \gamma_\mu (1 \pm \gamma_5) q_2$; α and β are color indices; q' denotes all the active quarks at the scale of $\mathcal{O}(m_b)$, i.e., $q' = u, d, c, s, b$; and $Q_{q'}$ is the electric charge of quark q' in the unit of $|e|$.

The Wilson coefficients $C_i(\mu)$, which summarize the physical contributions above the scale of μ , have been properly calculated at the next-to-leading order with the renormalization

group equation assisted perturbation theory [17]. Due to the presence of long-distance QCD effects and the entanglement of nonperturbative and perturbative shares, the main obstacle to evaluate the $B_q^{(*)}$ weak decays is the treatment of physical contributions below the scale of μ which are included in the HTME of local operators.

B. Hadronic matrix elements

Some phenomenological models have recently been developed to improve the sketchy treatment with naive factorization scheme [18, 19]. These models are generally based on the Lepage-Brodsky approach [20] and some power counting rules in parameters of α_s and Λ_{QCD}/m_Q (where α_s is the strong coupling, Λ_{QCD} is the QCD characteristic scale, and m_Q is the mass of a heavy quark), and express the HTME as a convolution integral of universal wave functions and hard scattering subamplitudes, such as the QCDF approach [9–11], pQCD approach [14–16], the soft and collinear effective theory [21–24], and so on, which have been extensively employed in the interpretation of the B weak decays. To wipe out the endpoint singularities appearing in the collinear approximation [9–11], it is suggested by the pQCD approach [14–16] that the transverse momentum k_T of valence quarks should be retaken, and a Sudakov factor should be introduced for each wave function to further suppress the soft contributions and make the hard scattering more perturbative. Finally, a decay amplitude is written as a multidimensional integral of many parts [15, 16], including the Wilson coefficients C_i , the heavy quark decay subamplitudes \mathcal{H} , and the universal wave functions Φ ,

$$\mathcal{A} \sim \sum_i \int \prod_j dk_j C_i(t) \mathcal{H}_i(t, k_j) \Phi_j(k_j) e^{-S_j}, \quad (7)$$

where t is a typical scale; k_j is the momentum of a valence quark; e^{-S_j} is a Sudakov factor.

C. Kinematic variables

The light-cone variables in the rest frame of the B^* meson are defined as follows.

$$p_{B^*} = p_1 = \frac{m_1}{\sqrt{2}}(1, 1, 0), \quad (8)$$

$$p_{\overline{D}} = p_2 = (p_2^+, p_2^-, 0), \quad (9)$$

$$p_D = p_3 = (p_3^-, p_3^+, 0), \quad (10)$$

$$k_i = x_i p_i + (0, 0, \vec{k}_{iT}), \quad (11)$$

$$p_i^\pm = (E_i \pm p)/\sqrt{2}, \quad (12)$$

$$\epsilon_{B^*}^\parallel = \frac{1}{\sqrt{2}}(-1, 1, 0), \quad (13)$$

$$s = 2 p_2 \cdot p_3, \quad (14)$$

$$t = 2 p_1 \cdot p_2 = 2 m_1 E_2, \quad (15)$$

$$u = 2 p_1 \cdot p_3 = 2 m_1 E_3, \quad (16)$$

$$s t + s u - t u - 4 m_1^2 p^2 = 0, \quad (17)$$

where the subscripts $i = 1, 2, 3$ of variables (energy E_i , momentum p_i and mass m_i) correspond to B^* , \bar{D} and D mesons, respectively; k_i is the momentum of the valence quark with the longitudinal momentum fraction x_i and the transverse momentum \vec{k}_{iT} ; $\epsilon_{B^*}^\parallel$ is the longitudinal polarization vector; p is the momentum of the final states; s , t and u are the Lorentz invariant parameters. The notation is displayed in Fig.2.

D. Wave functions

Wave functions are the basic input parameters with the pQCD approach. Although wave functions contain soft and nonperturbative contributions, they are universal, i.e., process independent. Wave functions and/or distribution amplitudes (DAs) determined by nonperturbative methods or extracted from data, can be employed here to make predictions.

Following the notations in Refs. [25–28], HTME of the diquark operators is defined as

$$\langle 0 | \bar{b}_i(0) q_j(z) | B^*(p, \epsilon^\parallel) \rangle = \frac{f_{B^*}}{4} \int d^4 k e^{-ik \cdot z} \left\{ \not{\epsilon}^\parallel \left[m_{B^*} \Phi_{B^*}^v(k) - \not{p} \Phi_{B^*}^t(k) \right] \right\}_{ji}, \quad (18)$$

$$\langle \bar{D}(p) | c_i(0) \bar{q}_j(z) | 0 \rangle = \frac{i f_D}{4} \int d^4 k e^{+ik \cdot z} \left\{ \gamma_5 \left[\not{p} \Phi_D^a(k) + m_{\bar{D}} \Phi_D^p(k) \right] \right\}_{ji}, \quad (19)$$

where f_{B^*} and f_D are decay constants; the wave functions $\Phi_{B^*}^v$ and $\Phi_{\bar{D}}^a$ are twist-2; and $\Phi_{B^*}^t$ and $\Phi_{\bar{D}}^p$ are twist-3. Due to the kinematic relation $\epsilon_{B^*}^\parallel \cdot p_i = 0$, the transversely polarized B^* meson contributes nothing to the amplitudes for the $B^* \rightarrow \bar{D}D$ decays. The expressions for DAs of the B^* and D mesons are [27, 28]

$$\phi_{B^*}^v(x) = A x \bar{x} \exp \left\{ - \frac{\bar{x} m_q^2 + x m_b^2}{8 \omega_1^2 x \bar{x}} \right\}, \quad (20)$$

$$\phi_{B^*}^t(x) = B (\bar{x} - x)^2 \exp\left\{-\frac{\bar{x} m_q^2 + x m_b^2}{8\omega_1^2 x \bar{x}}\right\}, \quad (21)$$

$$\phi_D^a(x) = C x \bar{x} \exp\left\{-\frac{\bar{x} m_q^2 + x m_c^2}{8\omega_2^2 x \bar{x}}\right\}, \quad (22)$$

$$\phi_D^p(x) = D \exp\left\{-\frac{\bar{x} m_q^2 + x m_c^2}{8\omega_2^2 x \bar{x}}\right\}, \quad (23)$$

where x and $\bar{x} (\equiv 1 - x)$ are the parton momentum fractions; ω_i determines the average transverse momentum of partons and $\omega_i \simeq m_i \alpha_s(m_i)$; parameters A, B, C, D are the normalization coefficients satisfying the conditions

$$\int_0^1 dx \phi_{B^*}^{v,t}(x) = 1, \quad (24)$$

$$\int_0^1 dx \phi_D^{a,p}(x) = 1. \quad (25)$$

In fact, there are many phenomenological models of DAs for the charmed meson, for example, some of them have been listed by Eq.(30) in Ref.[29]. One of the favorable models from the experimental data within the pQCD framework has the expression [29]

$$\phi_D(x) = 6 x \bar{x} \{1 + C_D(1 - 2x)\}, \quad (26)$$

where parameter $C_D = 0.5$ for the $D_{u,d}$ meson, and $C_D = 0.4$ for the D_s meson. In the actual calculation [29–32], there is no distinction between twist-2 and twist-3 DAs.

The shape lines of the normalized DAs $\phi_{B^*}^{v,t}(x)$ and $\phi_D^{a,p}(x)$ are illustrated in Fig.1. It is clearly seen from Fig.1 that (1) the shape lines of DAs in Eqs.(20)-(23) have a broad peak in the small x regions, which is generally consistent with an ansatz in which a light quark carries fewer parton momentum fractions than a heavy quark in a heavy-light system. (2) Due to the suppression from exponential functions, the DAs of Eqs.(20)-(23) converge quickly to zero at endpoint $x, \bar{x} \rightarrow 0$, which supplies the soft contributions with an effective cutoff. (3) The flavor symmetry breaking effects, and especially the distinction between different the twist DAs, are highlighted, compared with the nearly symmetric distribution Eq.(26).

E. Decay amplitudes

The Feynman diagrams for the $B^{*0} \rightarrow D^+ D^-$ decay with the pQCD approach are shown in Fig.2, including the factorizable emission topologies (a,b) where one gluon links with

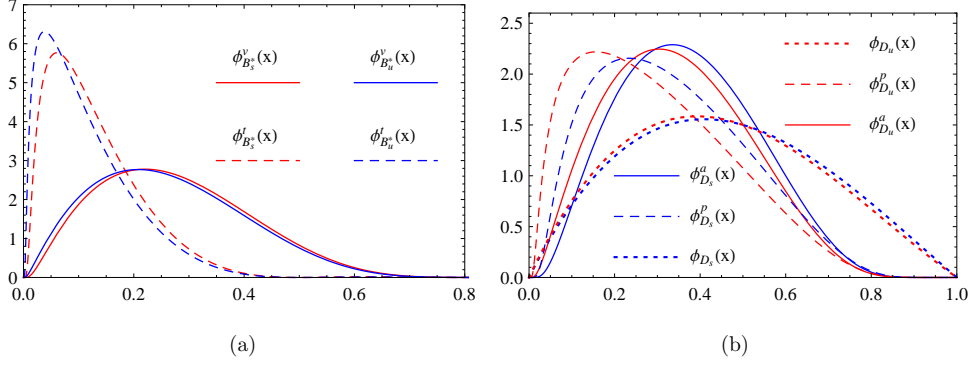


FIG. 1: The distributions of DAs $\phi_{B^{*0}}^{v,t}(x)$ [Eqs.(20,21)], $\phi_{D^{*0}}^{a,p}(x)$ [Eqs.(22,23)], and $\phi_D(x)$ [Eq.(26)].

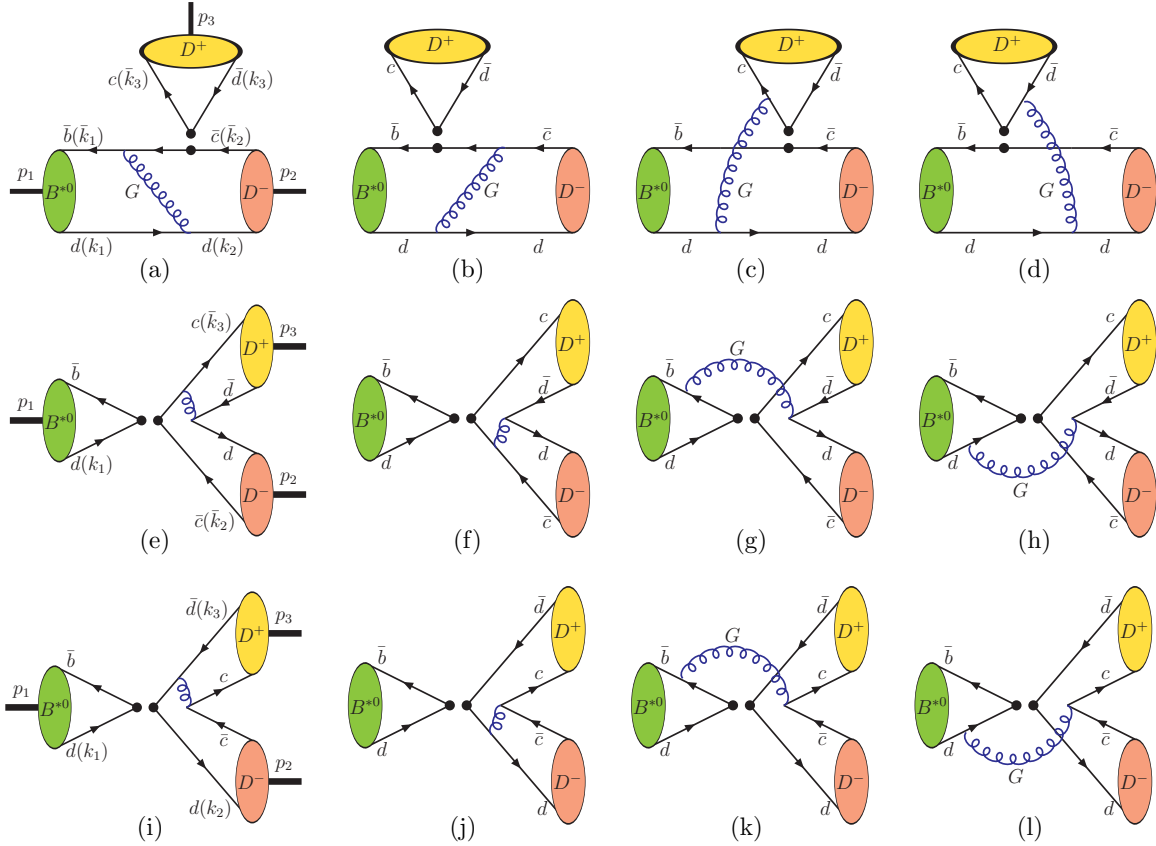


FIG. 2: Feynman diagrams for $B^{*0} \rightarrow D^{*+} D^{*0}$ decay, where (a,b) are the factorizable emission topologies, (c,d) are the nonfactorizable emission topologies, (e,f,i,j) are the factorizable annihilation topologies, and (g,h,k,l) are the nonfactorizable annihilation topologies.

the initial and the recoiled states, the nonfactorizable emission topologies (c,d) where one gluon is exchanged between the spectator quark and the emitted states, the factorizable annihilation topologies (e,f,i,j) where one gluon is conjoined with the final states, and the nonfactorizable annihilation topologies (g,h,k,l) where one gluon is transmitted between the

initial and the final states.

Generally, the amplitudes for the factorizable emission topologies in Fig.2(a,b) can be written as the D meson decay constant and the space-like $B^* \rightarrow D$ transition form factor, and the amplitudes for the factorizable annihilation topologies in Fig.2(e,f,i,j) can be written as the B^* meson decay constant and the time-like transition form factor between two charmed mesons. The amplitudes for the nonfactorizable topologies have more complicated structures, and can be written as the convolution integral of all participating meson wave functions. Compared with the contributions of the emission topologies in Fig.2(a-d), the contributions of the annihilation topologies in Fig.2(e-l) are assumed to be power suppressed, as stated in Ref.[10]. In addition, different topologies have different scales. The gluons of the emission topologies in Fig.2(a-d) are time-like, while the gluons of the annihilation topologies in Fig.2(e-l) are space-like. The gluon virtuality of creating a pair of heavy charm quarks from the vacuum for the annihilation topologies in Fig.2(i-l), $k_g^2 \geq (2m_c)^2$, should be much larger than that of producing a pair of light quarks for the annihilation topologies in Fig.2(e-h). Thus, it is not hard to figure out that the contributions of the annihilation topologies in Fig.2(i-l) might be very small relative to the others, because of the nature of the asymptotic freedom of the QCD at the ultrahigh energy.

After a straightforward calculation, the amplitudes for the $B_q^* \rightarrow \bar{D}D$ decays are expressed as below.

$$\begin{aligned}
& \mathcal{A}(B^{*+} \rightarrow \bar{D}^0 D_q^+) \\
&= \mathcal{F} \left\{ V_{cb}^* V_{cq} \left[a_1 \mathcal{A}_{a+b}^{LL} + C_2 \mathcal{A}_{c+d}^{LL} \right] + V_{ub}^* V_{uq} \left[a_1 \mathcal{A}_{i+j}^{LL} + C_2 \mathcal{A}_{k+l}^{LL} \right] \right. \\
&\quad \left. - V_{tb}^* V_{tq} \left[(a_4 + a_{10}) \mathcal{A}_{a+b+i+j}^{LL} + (a_6 + a_8) \mathcal{A}_{a+b}^{SP} \right. \right. \\
&\quad \left. \left. + (C_3 + C_9) \mathcal{A}_{c+d+k+l}^{LL} + (C_5 + C_7) \mathcal{A}_{c+d+k+l}^{SP} \right] \right\}, \tag{27}
\end{aligned}$$

$$\begin{aligned}
& \mathcal{A}(B_q^{*0} \rightarrow \bar{D}^0 D^0) \\
&= \mathcal{F} \left\{ V_{cb}^* V_{cq} \left[a_2 \mathcal{A}_{e+f}^{LL} + C_1 \mathcal{A}_{g+h}^{LL} \right] + V_{ub}^* V_{uq} \left[a_2 \mathcal{A}_{i+j}^{LL} + C_1 \mathcal{A}_{k+l}^{LL} \right] \right. \\
&\quad \left. - V_{tb}^* V_{tq} \left[(a_3 + a_9) \mathcal{A}_{e+f+i+j}^{LL} + (a_5 + a_7) \mathcal{A}_{e+f+i+j}^{LR} \right. \right. \\
&\quad \left. \left. + (C_4 + C_{10}) \mathcal{A}_{g+h+k+l}^{LL} + (C_6 + C_8) \mathcal{A}_{g+h+k+l}^{LR} \right] \right\}, \tag{28}
\end{aligned}$$

$$\begin{aligned}
& \mathcal{A}(B_q^{*0} \rightarrow D_q^- D_q^+) \\
= & \mathcal{F} \left\{ V_{cb}^* V_{cq} \left[a_1 \mathcal{A}_{a+b}^{LL} + C_2 \mathcal{A}_{c+d}^{LL} + a_2 \mathcal{A}_{e+f}^{LL} + C_1 \mathcal{A}_{g+h}^{LL} \right] \right. \\
& - V_{tb}^* V_{tq} \left[(a_4 + a_{10}) \mathcal{A}_{a+b}^{LL} + (a_6 + a_8) \mathcal{A}_{a+b}^{SP} + (a_3 + a_9) \mathcal{A}_{e+f}^{LL} \right. \\
& + (C_3 + C_9) \mathcal{A}_{c+d}^{LL} + (C_5 + C_7) \mathcal{A}_{c+d}^{SP} + (C_4 + C_{10}) \mathcal{A}_{g+h}^{LL} \\
& + (a_5 - \frac{1}{2} a_7) \mathcal{A}_{i+j}^{LR} + (C_5 - \frac{1}{2} C_7) \mathcal{A}_{k+l}^{SP} + (C_6 - \frac{1}{2} C_8) \mathcal{A}_{k+l}^{LR} \\
& + (a_5 + a_7) \mathcal{A}_{e+f}^{LR} + (a_3 + a_4 - \frac{1}{2} a_9 - \frac{1}{2} a_{10}) \mathcal{A}_{i+j}^{LL} \\
& \left. \left. + (C_6 + C_8) \mathcal{A}_{g+h}^{LR} + (C_3 + C_4 - \frac{1}{2} C_9 - \frac{1}{2} C_{10}) \mathcal{A}_{k+l}^{LL} \right] \right\}, \tag{29}
\end{aligned}$$

$$\begin{aligned}
& \mathcal{A}(B_d^{*0} \rightarrow D^- D_s^+) \\
= & \mathcal{F} \left\{ V_{cb}^* V_{cs} \left[a_1 \mathcal{A}_{a+b}^{LL} + C_2 \mathcal{A}_{c+d}^{LL} \right] - V_{tb}^* V_{ts} \left[(a_4 + a_{10}) \mathcal{A}_{a+b}^{LL} \right. \right. \\
& + (a_4 - \frac{1}{2} a_{10}) \mathcal{A}_{i+j}^{LL} + (C_3 - \frac{1}{2} C_9) \mathcal{A}_{k+l}^{LL} + (C_5 - \frac{1}{2} C_7) \mathcal{A}_{k+l}^{SP} \\
& \left. \left. + (a_6 + a_8) \mathcal{A}_{a+b}^{SP} + (C_3 + C_9) \mathcal{A}_{c+d}^{LL} + (C_5 + C_7) \mathcal{A}_{c+d}^{SP} \right] \right\}, \tag{30}
\end{aligned}$$

$$\begin{aligned}
& \mathcal{A}(B_s^{*0} \rightarrow D_s^- D^+) \\
= & \mathcal{F} \left\{ V_{cb}^* V_{cd} \left[a_1 \mathcal{A}_{a+b}^{LL} + C_2 \mathcal{A}_{c+d}^{LL} \right] - V_{tb}^* V_{td} \left[(a_4 + a_{10}) \mathcal{A}_{a+b}^{LL} \right. \right. \\
& + (a_4 - \frac{1}{2} a_{10}) \mathcal{A}_{i+j}^{LL} + (C_3 - \frac{1}{2} C_9) \mathcal{A}_{k+l}^{LL} + (C_5 - \frac{1}{2} C_7) \mathcal{A}_{k+l}^{SP} \\
& \left. \left. + (a_6 + a_8) \mathcal{A}_{a+b}^{SP} + (C_3 + C_9) \mathcal{A}_{c+d}^{LL} + (C_5 + C_7) \mathcal{A}_{c+d}^{SP} \right] \right\}, \tag{31}
\end{aligned}$$

$$\begin{aligned}
& \mathcal{A}(B_d^{*0} \rightarrow D_s^- D_s^+) \\
= & \mathcal{F} \left\{ V_{cb}^* V_{cd} \left[a_2 \mathcal{A}_{e+f}^{LL} + C_1 \mathcal{A}_{g+h}^{LL} \right] - V_{tb}^* V_{td} \left[(a_3 + a_9) \mathcal{A}_{e+f}^{LL} \right. \right. \\
& + (a_5 + a_7) \mathcal{A}_{e+f}^{LR} + (C_4 + C_{10}) \mathcal{A}_{g+h}^{LL} + (C_6 + C_8) \mathcal{A}_{g+h}^{LR} \\
& + (a_3 - \frac{1}{2} a_9) \mathcal{A}_{i+j}^{LL} + (C_4 - \frac{1}{2} C_{10}) \mathcal{A}_{k+l}^{LL} \\
& \left. \left. + (a_5 - \frac{1}{2} a_7) \mathcal{A}_{i+j}^{LR} + (C_6 - \frac{1}{2} C_8) \mathcal{A}_{k+l}^{LR} \right] \right\}, \tag{32}
\end{aligned}$$

$$\begin{aligned}
& \mathcal{A}(B_s^{*0} \rightarrow D^- D^+) \\
= & \mathcal{F} \left\{ V_{cb}^* V_{cs} \left[a_2 \mathcal{A}_{e+f}^{LL} + C_1 \mathcal{A}_{g+h}^{LL} \right] - V_{tb}^* V_{ts} \left[(a_3 + a_9) \mathcal{A}_{e+f}^{LL} \right. \right. \\
& + (a_5 + a_7) \mathcal{A}_{e+f}^{LR} + (C_4 + C_{10}) \mathcal{A}_{g+h}^{LL} + (C_6 + C_8) \mathcal{A}_{g+h}^{LR} \\
& + (a_3 - \frac{1}{2} a_9) \mathcal{A}_{i+j}^{LL} + (C_4 - \frac{1}{2} C_{10}) \mathcal{A}_{k+l}^{LL} \\
& \left. \left. + (a_5 - \frac{1}{2} a_7) \mathcal{A}_{i+j}^{LR} + (C_6 - \frac{1}{2} C_8) \mathcal{A}_{k+l}^{LR} \right] \right\}, \tag{33}
\end{aligned}$$

$$\mathcal{F} = \sqrt{2} G_F \frac{\pi C_F}{N_c} f_{B_q^*} f_{\bar{D}} f_D m_1 (\epsilon_{B_q^*} p_{\bar{D}}), \quad (34)$$

where C_i is the Wilson coefficient; the parameter a_i is defined as

$$a_i = \begin{cases} C_i + C_{i+1}/N_c & \text{for odd } i; \\ C_i + C_{i-1}/N_c & \text{for even } i, \end{cases} \quad (35)$$

and $\mathcal{A}_{m_1+m_2+\dots}^n$ is an abbreviation for $\mathcal{A}_{m_1}^n + \mathcal{A}_{m_2}^n + \dots$, where the subscript m_i corresponds to one of indices of Fig.2; the superscript n refers to three possible Dirac structures $\Gamma_1 \otimes \Gamma_2$ of the operators $(\bar{q}_1 q_2)_{\Gamma_1} (\bar{q}_3 q_4)_{\Gamma_2}$, namely $n = LL$ for $(V - A) \otimes (V - A)$, $n = LR$ for $(V - A) \otimes (V + A)$, and $n = SP$ for $-2(S - P) \otimes (S + P)$. The explicit expressions of the building blocks $\mathcal{A}_{m_i}^n$ are collected in Appendix.

III. NUMERICAL RESULTS AND DISCUSSION

In the rest frame of the B_q^* meson, the branching ratio is defined as

$$\mathcal{B}r = \frac{1}{24\pi} \frac{p}{m_{B_q^*}^2 \Gamma_{B_q^*}} |\mathcal{A}(B_q^* \rightarrow \bar{D}D)|^2, \quad (36)$$

where $\Gamma_{B_q^*}$ is the full decay width of the B_q^* meson.

TABLE I: The numerical values of the input parameters.

CKM parameter ^a [1]			
$\lambda = 0.22506 \pm 0.00050$,	$A = 0.811 \pm 0.026$,	$\bar{\rho} = 0.124_{-0.018}^{+0.019}$,	$\bar{\eta} = 0.356 \pm 0.011$;
mass and decay constant			
$m_{B_s^*} = 5415.4_{-1.5}^{+1.8}$ MeV [1],	$f_{B_s^*} = 213 \pm 7$ MeV [33],	$\Lambda_{\text{QCD}}^{(5)} = 210 \pm 14$ MeV [1],	
$m_{B_{u,d}^*} = 5324.65 \pm 0.25$ MeV [1],	$f_{B_{u,d}^*} = 175 \pm 6$ MeV [33],	$\Lambda_{\text{QCD}}^{(4)} = 292 \pm 16$ MeV [1],	
$m_{D_s} = 1968.27 \pm 0.10$ MeV [1],	$f_{D_s} = 249.0 \pm 1.2$ MeV [1],	$m_b = 4.78 \pm 0.06$ GeV [1],	
$m_{D_d} = 1869.58 \pm 0.09$ MeV [1],	$f_{D_{u,d}} = 211.9 \pm 1.1$ MeV [1],	$m_c = 1.67 \pm 0.07$ GeV [1],	
$m_{D_u} = 1864.83 \pm 0.05$ MeV [1],	$m_{u,d} \simeq 0.31$ GeV [34],	$m_s \simeq 0.51$ GeV [34].	

^aThe relations between the CKM parameters (ρ, η) and $(\bar{\rho}, \bar{\eta})$ are [1]: $(\rho + i\eta) = \frac{\sqrt{1 - A^2 \lambda^4} (\bar{\rho} + i\bar{\eta})}{\sqrt{1 - \lambda^2 [1 - A^2 \lambda^4 (\bar{\rho} + i\bar{\eta})]}}$.

The numerical values of some input parameters are listed in Table I, where if it is not specified explicitly, their central values will be fixed as the default inputs. Besides, the full

decay width of the B_q^* meson, $\Gamma_{B_q^*}$, is also an essential parameter. Unfortunately, an experimental measurement on $\Gamma_{B_q^*}$ is unavailable now, because the soft photon from the $B_q^* \rightarrow B_q \gamma$ process is usually beyond the detection capability of electromagnetic calorimeters sitting at existing high energy colliders. It is well known that the electromagnetic radiation process $B_q^* \rightarrow B_q \gamma$ dominates the decay of the B_q^* meson. So, for the time being, the full decay width will be approximated by the radiative partial width, i.e., $\Gamma_{B_q^*} \simeq \Gamma(B_q^* \rightarrow B_q \gamma)$. At present, the information on $\Gamma(B_q^* \rightarrow B_q \gamma)$ comes mainly from theoretical estimation. Theoretically, the partial decay width of the M1 transition (spin-flip) process has the expression [35, 36]

$$\Gamma(B_q^* \rightarrow B_q \gamma) = \frac{4}{3} \alpha k_\gamma^3 \mu_h^2, \quad (37)$$

where α is the fine structure constant; $k_\gamma = (m_{B_q^*}^2 - m_{B_q}^2)/2m_{B_q^*}$ is the photon momentum in the rest frame of the B_q^* meson; μ_h is the M1 moment of the B_q^* meson. There are plenty of theoretical predictions on $\Gamma(B_q^* \rightarrow B_q \gamma)$, for example, the numbers in Table 7 in Ref.[35] and Tables 3 and 4 in Ref.[36], but these estimation suffer from large uncertainties due to our insufficient understanding on the M1 moments of mesons. In principle, the M1 moment of a meson should be a combination of the M1 moments of the constituent quark and antiquark. For a heavy-light meson, the M1 moment of a heavy quark might be negligible relative to the M1 moment of a light quark, because it is widely assumed that the mass of a heavy quark is usually much larger than the mass of a light quark, and that the M1 moment is inversely proportional to the mass of a charged particle. With the M1 moment relations among light u , d , s quarks, $|\mu_u| > |\mu_d| > |\mu_s|$ [34], one could expect to have $\Gamma(B_u^* \rightarrow B_u \gamma) > \Gamma(B_d^* \rightarrow B_d \gamma) > \Gamma(B_s^* \rightarrow B_s \gamma)$, and so $\Gamma_{B_u^*} > \Gamma_{B_d^*} > \Gamma_{B_s^*}$. Of course, more details about the width $\Gamma_{B_q^*}$ is beyond the scope of this paper. In our calculation, in order to give a quantitative estimation of the branching ratios for the $B^* \rightarrow \overline{D}D$ decays, we will fix

$$\Gamma_{B_u^*} \sim \Gamma(B_u^* \rightarrow B_u \gamma) \sim 450 \text{ eV}, \quad (38)$$

$$\Gamma_{B_d^*} \sim \Gamma(B_d^* \rightarrow B_d \gamma) \sim 150 \text{ eV}, \quad (39)$$

$$\Gamma_{B_s^*} \sim \Gamma(B_s^* \rightarrow B_s \gamma) \sim 100 \text{ eV}, \quad (40)$$

which is basically consistent with the recent results in Refs.[35, 36].

In order to investigate the effects from different DA models, we explore three scenarios,

- Scenario I: $\phi_{B^*}^v = \text{Eq.}(20)$, $\phi_{B^*}^t = \text{Eq.}(21)$, $\phi_{D,D}^a = \text{Eq.}(22)$ and $\phi_{D,D}^p = \text{Eq.}(23)$.

- Scenario II: $\phi_{B^*}^v = \phi_{B^*}^t = \text{Eq.}(20)$, and $\phi_{\bar{D},D}^a = \phi_{\bar{D},D}^p = \text{Eq.}(22)$.
- Scenario III: $\phi_{B^*}^v = \phi_{B^*}^t = \text{Eq.}(20)$, $\phi_{\bar{D},D}^a = \phi_{\bar{D},D}^p = \text{Eq.}(26)$.

Our numerical results are presented in Table II, where the uncertainties come from the typical scale $(1\pm 0.1)t_i$, mass m_c and m_b , and the CKM parameters, respectively. The following are some comments.

TABLE II: The branching ratios for the $B^* \rightarrow \bar{D}D$ decays, where the theoretical uncertainties come from scale $(1\pm 0.1)t_i$, mass m_c and m_b , and the CKM parameters, respectively; the numbers in columns correspond to different DA scenarios.

	class	I	II	III
$\mathcal{B}r(B_u^{*+} \rightarrow \bar{D}_u^0 D_d^+) \times 10^{11}$	B	$7.65^{+1.81+0.04+0.62}_{-0.68-0.78-0.59}$	$2.21^{+0.40+0.17+0.18}_{-0.17-0.21-0.17}$	$1.24^{+0.20+0.15+0.10}_{-0.09-0.16-0.09}$
$\mathcal{B}r(B_u^{*+} \rightarrow \bar{D}_u^0 D_s^+) \times 10^9$	A	$1.89^{+0.45+0.01+0.14}_{-0.17-0.19-0.13}$	$0.57^{+0.11+0.04+0.04}_{-0.05-0.05-0.04}$	$0.31^{+0.05+0.04+0.02}_{-0.02-0.04-0.02}$
$\mathcal{B}r(B_d^{*0} \rightarrow D_d^- D_s^+) \times 10^9$	A	$5.68^{+1.36+0.01+0.42}_{-0.51-0.54-0.40}$	$1.72^{+0.33+0.13+0.13}_{-0.14-0.17-0.12}$	$0.94^{+0.16+0.12+0.07}_{-0.07-0.12-0.07}$
$\mathcal{B}r(B_s^{*0} \rightarrow D_s^- D_d^+) \times 10^{10}$	B	$6.34^{+1.40+0.07+0.51}_{-0.54-0.45-0.49}$	$2.09^{+0.38+0.12+0.17}_{-0.16-0.18-0.16}$	$1.15^{+0.19+0.12+0.09}_{-0.08-0.13-0.09}$
$\mathcal{B}r(B_d^{*0} \rightarrow D_d^- D_d^+) \times 10^{10}$	B	$2.27^{+0.55+0.00+0.18}_{-0.21-0.21-0.17}$	$0.68^{+0.12+0.05+0.05}_{-0.05-0.06-0.05}$	$0.39^{+0.06+0.05+0.03}_{-0.03-0.05-0.03}$
$\mathcal{B}r(B_s^{*0} \rightarrow D_s^- D_s^+) \times 10^8$	A	$1.51^{+0.34+0.03+0.11}_{-0.13-0.12-0.11}$	$0.53^{+0.10+0.03+0.04}_{-0.04-0.04-0.04}$	$0.30^{+0.05+0.03+0.02}_{-0.02-0.03-0.02}$
$\mathcal{B}r(B_d^{*0} \rightarrow \bar{D}_u^0 D_u^0) \times 10^{14}$	D	$1.53^{+0.73+1.45+0.19}_{-0.61-0.21-0.17}$	$0.43^{+0.14+0.53+0.07}_{-0.12-0.34-0.06}$	$4.10^{+0.12+0.26+0.48}_{-0.02-0.25-0.44}$
$\mathcal{B}r(B_d^{*0} \rightarrow D_s^- D_s^+) \times 10^{13}$	D	$1.11^{+0.16+0.22+0.09}_{-0.19-0.20-0.09}$	$0.99^{+0.06+0.17+0.08}_{-0.06-0.18-0.08}$	$0.66^{+0.03+0.04+0.05}_{-0.02-0.04-0.05}$
$\mathcal{B}r(B_s^{*0} \rightarrow \bar{D}_u^0 D_u^0) \times 10^{13}$	C	$7.57^{+3.07+6.57+0.58}_{-2.52-1.66-0.55}$	$1.97^{+0.67+2.71+0.15}_{-0.58-1.68-0.15}$	$10.35^{+0.64+1.00+0.79}_{-0.39-1.01-0.76}$
$\mathcal{B}r(B_s^{*0} \rightarrow D_d^- D_d^+) \times 10^{13}$	C	$7.62^{+3.07+6.51+0.57}_{-2.53-1.61-0.55}$	$1.99^{+0.67+2.64+0.15}_{-0.58-1.67-0.14}$	$10.41^{+0.60+0.98+0.77}_{-0.37-1.00-0.74}$

(1) Generally, the $B^* \rightarrow \bar{D}D$ decay modes may be divided into four classes. The tree contributions of classes A, B, C, D are proportional to the factors of $V_{cb}^* V_{cs} a_1 \sim A\lambda^2 a_1$, $V_{cb}^* V_{cd} a_1 \sim A\lambda^3 a_1$, $V_{cb}^* V_{cs} a_2 \sim A\lambda^2 a_2$, $V_{cb}^* V_{cd} a_2 \sim A\lambda^3 a_2$, respectively. Classes C and D are pure annihilation processes. There is a clear hierarchy of branching ratios, i.e., $\mathcal{B}r(\text{class A}) \gtrsim 10^{-9}$, $\mathcal{B}r(\text{class B}) \gtrsim 10^{-11}$, $\mathcal{B}r(\text{class C}) \gtrsim 10^{-13}$, $\mathcal{B}r(\text{class D}) \lesssim 10^{-13}$.

In addition, for each class, the magnitude relations between the decay constants $f_{B_s^*} > f_{B_{u,d}^*}$ and $f_{D_s} > f_{D_{u,d}}$, and relations among the decay widths $\Gamma_{B_s^*} < \Gamma_{B_d^*} < \Gamma_{B_u^*}$, result in the size relations among the branching ratios, i.e.,

$$\mathcal{B}r(B_s^{*0} \rightarrow D_s^- D_s^+) > \mathcal{B}r(B_d^{*0} \rightarrow D_d^- D_s^+) > \mathcal{B}r(B_u^{*+} \rightarrow \bar{D}_u^0 D_s^+), \quad (41)$$

$$\mathcal{B}r(B_s^{*0} \rightarrow D_s^- D_d^+) > \mathcal{B}r(B_d^{*0} \rightarrow D_d^- D_d^+) > \mathcal{B}r(B_u^{*+} \rightarrow \overline{D}_u^0 D_d^+), \quad (42)$$

$$\mathcal{B}r(B_d^{*0} \rightarrow D_s^- D_s^+) > \mathcal{B}r(B_d^{*0} \rightarrow \overline{D}_u^0 D_u^0). \quad (43)$$

(2) Due to the isospin symmetry, there are some approximate relations among the branching ratios, for example,

$$\frac{\mathcal{B}r(B_d^{*0} \rightarrow D_d^- D_s^+)}{\mathcal{B}r(B_u^{*+} \rightarrow \overline{D}_u^0 D_s^+)} \approx \frac{\Gamma_{B_u^*}}{\Gamma_{B_d^*}} \approx 3, \quad (44)$$

$$\frac{\mathcal{B}r(B_d^{*0} \rightarrow D_d^- D_d^+)}{\mathcal{B}r(B_u^{*+} \rightarrow \overline{D}_u^0 D_d^+)} \approx \frac{\Gamma_{B_u^*}}{\Gamma_{B_d^*}} \approx 3, \quad (45)$$

$$\frac{\mathcal{B}r(B_s^{*0} \rightarrow \overline{D}_u^0 D_u^0)}{\mathcal{B}r(B_s^{*0} \rightarrow D_d^- D_d^+)} \approx 1. \quad (46)$$

In addition, there are some other approximate relations, for example,

$$\frac{\mathcal{B}r(B_u^{*+} \rightarrow \overline{D}_u^0 D_s^+)}{\mathcal{B}r(B_u^{*+} \rightarrow \overline{D}_u^0 D_d^+)} \approx \frac{f_{D_s}^2 |V_{cs}|^2}{f_{D_d}^2 |V_{cd}|^2}, \quad (47)$$

$$\frac{\mathcal{B}r(B_d^{*0} \rightarrow D_d^- D_s^+)}{\mathcal{B}r(B_d^{*0} \rightarrow D_d^- D_d^+)} \approx \frac{f_{D_s}^2 |V_{cs}|^2}{f_{D_d}^2 |V_{cd}|^2}, \quad (48)$$

$$\frac{\mathcal{B}r(B_s^{*0} \rightarrow D_s^- D_s^+)}{\mathcal{B}r(B_s^{*0} \rightarrow D_s^- D_d^+)} \approx \frac{f_{D_s}^2 |V_{cs}|^2}{f_{D_d}^2 |V_{cd}|^2}. \quad (49)$$

(3) Our study shows that (i) both the emission topologies and the annihilation topologies contribute to the decay channels of Classes A and B. Furthermore, the contributions from the emission topologies are dominant over those from the annihilation topologies. (ii) For the pure annihilation decay channels of Classes C and D, the factorizable contributions are color-suppressed, so the nonfactorizable contributions are the main ones. In addition, the interferences among different topologies are important. (iii) Compared with the contributions of the tree operators, the contributions of the penguin operators are small because of the suppression from the small Wilson coefficients. The contributions of the topologies in Fig.2(i-l) are much less than those of the topologies in Fig.2(e-h). (iv) For the decay channels with the final states $\overline{D}_q D_q$, the contribution of the factorizable annihilation topology in Fig.2(e) [Fig.2(i)] is the same magnitude as that in Fig.2(f) [Fig.2(j)] due to the flavor symmetry. (v) The interferences between factorizable topologies in Fig.2(e) and Fig.2(f) [Fig.2(i) and Fig.2(j)] are constructive, while the interferences between nonfactorizable topologies in Fig.2(g) and Fig.2(h) [Fig.2(k) and Fig.2(l)] are destructive.

TABLE III: The fractions (in the unit of %) of the different b -hadron species.

channels	$(b\bar{s})(\bar{b}s)$	$B_s^{*0}\bar{B}_s^{*0}$	$B_s^{*0}\bar{B}_s^0 + \text{c.c.}$	$\begin{matrix} (b\bar{u})(\bar{b}u) \\ +(b\bar{d})(\bar{b}d) \end{matrix}$	$B^*\bar{B}^*$	$B^*\bar{B} + \text{c.c.}$	$B^*\bar{B}\pi + \text{c.c.}$	$B^*\bar{B}^*\pi$
fractions	\mathcal{B}_s	$\mathcal{B}_{B_s^{*0}\bar{B}_s^{*0}}$	$\mathcal{B}_{B_s^{*0}\bar{B}_s^0}$	$\mathcal{B}_u + \mathcal{B}_d$	$\mathcal{B}_{B^*\bar{B}^*}$			
$\Upsilon(5S)$ [37]	$19.5_{-2.3}^{+3.0}$	17.6 ± 2.8	1.4 ± 0.7	73.7 ± 6.0	37.5 ± 3.7	13.7 ± 1.7	7.3 ± 2.4	1.0 ± 1.5
Tevatron [38]	10.0 ± 1.0				70.0 ± 4.0			

(4) The $B_s^{*0} \rightarrow D_s^- D_s^+$, $B_d^{*0} \rightarrow D_d^- D_d^+$, $B_u^{*+} \rightarrow \bar{D}_u^0 D_s^+$ decays, belonging to class A, have relatively large branching ratios, $\mathcal{B}r(\text{class A}) \gtrsim 10^{-9}$. The numbers of the B_q^* mesons in a data sample can be estimated by

$$N(B_q^*) = \mathcal{L}_{\text{int}} \times \sigma_{b\bar{b}} \times \mathcal{B}_q \times \frac{\mathcal{B}_{B_q^*}}{\mathcal{B}_q}, \quad (50)$$

$$\mathcal{B}_{B_q^*} = 2 \times \mathcal{B}_{B_q^* \bar{B}_q^*} + 2 \times \mathcal{B}_{B_q^* \bar{B}_q^* \pi} + \mathcal{B}_{B_q^* \bar{B}_q^* \text{c.c.}} + \mathcal{B}_{B_q^* \bar{B}_q^* \pi \text{c.c.}} + \dots, \quad (51)$$

where \mathcal{L}_{int} is the integrated luminosity, $\sigma_{b\bar{b}}$ denotes the $b\bar{b}$ pair production cross section, \mathcal{B}_q refers to the fragmentation fraction of $(b\bar{q})(\bar{b}q)$ events, and $\mathcal{B}_{B_q^* \bar{B}_q^*}$, $\mathcal{B}_{B_q^* \bar{B}_q^* X}$, ... represent the production fractions of specific modes (see Table III). With a large production cross section of the process $e^+e^- \rightarrow b\bar{b}$ at the $\Upsilon(5S)$ peak $\sigma_{b\bar{b}} = (0.340 \pm 0.016)$ nb [37] and a high luminosity $8 \times 10^{35} \text{ cm}^{-2} \text{ s}^{-1}$ at the forthcoming SuperKEKB [39], it is expected that some 3.3×10^9 $B_{u,d}^*$ and 1.2×10^9 B_s^* mesons could be available per 10 ab^{-1} $\Upsilon(5S)$ dataset, corresponding to a few events of the $B_d^{*0} \rightarrow D_d^- D_d^+$ and $B_u^{*+} \rightarrow \bar{D}_u^0 D_s^+$ decays and dozens of the $B_s^{*0} \rightarrow D_s^- D_s^+$ decay. At high energy hadron colliders, for example, with a visible b -hadron cross section at the LHCb $\sigma_{b\bar{b}} \sim 100 \mu\text{b}$ [1, 40], a similar ratio \mathcal{B}_q at Tevatron and a similar ratio $\mathcal{B}_{B_q^*}/\mathcal{B}_q$ at $\Upsilon(5S)$, some 9.2×10^{13} $B_{u,d}^*$ and 1.9×10^{13} B_s^* events per ab^{-1} dataset should be available at the LHCb, corresponding to more than 10^5 (class A) $B_s^{*0} \rightarrow D_s^- D_s^+$, $B_d^{*0} \rightarrow D_d^- D_d^+$, and $B_u^{*+} \rightarrow \bar{D}_u^0 D_s^+$ decay events and over 10^4 (class B) $B_s^{*0} \rightarrow D_s^- D_d^+$, $B_d^{*0} \rightarrow D_d^- D_d^+$, $B_u^{*+} \rightarrow \bar{D}_u^0 D_d^+$ decay events, which are measurable at the future LHCb experiments. However, the search for pure annihilation processes (classes C and D) at LHC and SuperKEKB should still be very challenging.

(5) Compared with the branching ratios $\gtrsim 10^{-5}$ for the $B \rightarrow \bar{D}D$ decays [1, 30], the branching ratios for the $B^* \rightarrow \bar{D}D$ decays are smaller by at least three orders of magnitude. This fact might imply that the background from the $B^* \rightarrow \bar{D}D$ decays could be safely neglected when one analyzes the $B \rightarrow \bar{D}D$ decays, but not vice versa, i.e., one of main

pollution backgrounds for the $B^* \rightarrow \overline{D}D$ decays would come from the $B \rightarrow \overline{D}D$ decays, even if the invariant mass of the $\overline{D}D$ meson pair could be used to distinguish the B^* meson from the B meson experimentally.

(6) For the B_q^* decays of classes A and B, our estimation of the branching ratios agrees well with that based on the naive factorization approach [4]. One of the important reasons is that these processes are all a_1 -dominated (color favored), and in general, insensitive to nonfactorizable corrections to the HTME. Of course, one fact is clear that there are many theoretical uncertainties, especially, regarding the discrepancy among different DA scenarios, which results from our uncertain knowledge of the long-distance QCD effects and the underlying dynamics of low energy hadron interactions. Moreover, as aforementioned, there are large uncertainties of the decay width $\Gamma_{B_q^*}$. With a different value of $\Gamma_{B_q^*}$, the branching ratios in Table II should be multiplied by the factors of $450 \text{ eV}/\Gamma_{B_u^*}$, $150 \text{ eV}/\Gamma_{B_d^*}$, $100 \text{ eV}/\Gamma_{B_s^*}$ for the B_u^* , B_d^* , B_s^* decays, respectively. In addition, many other factors, such as the final state interactions, models for the B^* and D meson wave functions^b, higher order corrections to the HTME, and so on, are not carefully scrutinized here, but deserve much dedicated study. Our estimation may be just an order of magnitude.

IV. SUMMARY

With the running LHC and the forthcoming SuperKEKB, a large amount of B^* data should be in stock soon, which will make it seemingly possible to explore the B^* weak decays experimentally. A theoretical study is necessary in order to offer a timely reference, and is helpful in clearing up some of puzzles surrounding heavy meson weak decays. In this paper, we investigated the $B^* \rightarrow \overline{D}D$ decays with the phenomenological pQCD approach. It is found that the $B_s^{*0} \rightarrow D_s^- D_s^+$, $B_d^{*0} \rightarrow D_d^- D_s^+$, and $B_u^{*+} \rightarrow \overline{D}_u^0 D_s^+$ decays have branching ratios $\gtrsim 10^{-9}$, and will be promisingly accessible at the future high luminosity experiments, with help of a sophisticated experimental analytical technique to effectively suppress or

^b In principle, one can do a global fit on the B^* and D meson wave functions with experimental measurements in the future, analogous to that with the χ^2 method in Ref.[29]. The fitting will be a very time-consuming work, because the amplitudes for the $B^* \rightarrow \overline{D}D$ decays are expressed as the multidimensional integral with the pQCD approach. In addition, there is no measurement report on the $B^* \rightarrow \overline{D}D$ decays at the moment.

exclude the background from the $B \rightarrow \bar{D}D$ decays.

Acknowledgments

The work is supported by the National Natural Science Foundation of China (Grant Nos. U1632109, 11547014 and 11475055).

Appendix A: Amplitude building blocks for $B^* \rightarrow \bar{D}D$ decays

$$\begin{aligned} \mathcal{A}_a^{LL} &= \int_0^1 dx_1 \int_0^1 dx_2 \int_0^\infty b_1 db_1 \int_0^\infty b_2 db_2 \alpha_s(t_a) H_{ef}(\alpha_e, \beta_a, b_1, b_2) \\ &\quad \times E_{ef}(t_a) \phi_{B^*}^v(x_1) \left\{ \phi_D^a(x_2) (m_1^2 \bar{x}_2 + m_3^2 x_2) + \phi_D^p(x_2) m_2 m_b \right\}, \end{aligned} \quad (\text{A1})$$

$$\begin{aligned} \mathcal{A}_a^{SP} &= -2 m_3 \int_0^1 dx_1 \int_0^1 dx_2 \int_0^\infty b_1 db_1 \int_0^\infty b_2 db_2 H_{ef}(\alpha_e, \beta_a, b_1, b_2) \\ &\quad \times \alpha_s(t_a) E_{ef}(t_a) \phi_{B^*}^v(x_1) \left\{ \phi_D^a(x_2) m_b + \phi_D^p(x_2) m_2 x_2 \right\}, \end{aligned} \quad (\text{A2})$$

$$\begin{aligned} \mathcal{A}_b^{LL} &= \int_0^1 dx_1 \int_0^1 dx_2 \int_0^\infty b_1 db_1 \int_0^\infty b_2 db_2 \alpha_s(t_b) H_{ef}(\alpha_e, \beta_a, b_2, b_1) \\ &\quad \times E_{ef}(t_b) \left\{ \phi_{B^*}^t(x_1) \left[\phi_D^p(x_2) 2 m_1 m_2 \bar{x}_1 - \phi_D^a(x_2) m_1 m_c \right] \right. \\ &\quad \left. + \phi_{B^*}^v(x_1) \left[\phi_D^p(x_2) 2 m_2 m_c - \phi_D^a(x_2) (m_2^2 \bar{x}_1 + m_3^2 x_1) \right] \right\}, \end{aligned} \quad (\text{A3})$$

$$\begin{aligned} \mathcal{A}_b^{SP} &= 2 m_3 \int_0^1 dx_1 \int_0^1 dx_2 \int_0^\infty b_1 db_1 \int_0^\infty b_2 db_2 \alpha_s(t_b) H_{ef}(\alpha_e, \beta_a, b_2, b_1) \\ &\quad \times E_{ef}(t_b) \left\{ \phi_{B^*}^v(x_1) \left[\phi_D^a(x_2) m_c - \phi_D^p(x_2) 2 m_2 \right] + \phi_{B^*}^t(x_1) \phi_D^a(x_2) m_1 x_1 \right\}, \end{aligned} \quad (\text{A4})$$

$$\begin{aligned} \mathcal{A}_c^{LL} &= \frac{1}{N_c} \int_0^1 dx_1 \int_0^1 dx_2 \int_0^1 dx_3 \int_0^\infty db_1 \int_0^\infty b_2 db_2 \int_0^\infty b_3 db_3 \alpha_s(t_c) E_n(t_c) \\ &\quad \times H_{en}(\alpha_e, \beta_c, b_3, b_2, b_1) \left\{ \phi_{B^*}^t(x_1) \phi_D^p(x_2) \phi_D^a(x_3) m_1 m_2 (x_1 - x_2) \right. \\ &\quad \left. + \phi_{B^*}^v(x_1) \phi_D^a(x_2) \left[\phi_D^a(x_3) s(x_2 - \bar{x}_3) - \phi_D^p(x_3) m_3 m_c \right] \right\}, \end{aligned} \quad (\text{A5})$$

$$\begin{aligned} \mathcal{A}_c^{SP} &= \frac{1}{N_c} \int_0^1 dx_1 \int_0^1 dx_2 \int_0^1 dx_3 \int_0^\infty db_1 \int_0^\infty b_2 db_2 \int_0^\infty b_3 db_3 H_{en}(\alpha_e, \beta_c, b_3, b_2, b_1) \\ &\quad \times E_n(t_c) \alpha_s(t_c) \left\{ \phi_{B^*}^v(x_1) \phi_D^p(x_2) m_2 \left[\phi_D^p(x_3) m_3 (x_2 - \bar{x}_3) - \phi_D^a(x_3) m_c \right] \right. \\ &\quad \left. + \phi_{B^*}^t(x_1) \phi_D^a(x_2) m_1 \left[\phi_D^a(x_3) m_c + \phi_D^p(x_3) m_3 (\bar{x}_3 - x_1) \right] \right\}, \end{aligned} \quad (\text{A6})$$

$$\begin{aligned}
\mathcal{A}_d^{LL} &= \frac{1}{N_c} \int_0^1 dx_1 \int_0^1 dx_2 \int_0^1 dx_3 \int_0^\infty db_1 \int_0^\infty b_2 db_2 \int_0^\infty b_3 db_3 \alpha_s(t_d) E_n(t_d) \\
&\times H_{en}(\alpha_e, \beta_d, b_3, b_2, b_1) \phi_D^a(x_3) \left\{ \phi_{B^*}^t(x_1) \phi_D^p(x_2) m_1 m_2 (x_1 - x_2) \right. \\
&\quad \left. + \phi_{B^*}^v(x_1) \phi_D^a(x_2) (2 m_2^2 x_2 + s x_3 - t x_1) \right\}, \tag{A7}
\end{aligned}$$

$$\begin{aligned}
\mathcal{A}_d^{SP} &= \frac{1}{N_c} \int_0^1 dx_1 \int_0^1 dx_2 \int_0^1 dx_3 \int_0^\infty db_1 \int_0^\infty b_2 db_2 \int_0^\infty b_3 db_3 \alpha_s(t_d) E_n(t_d) \\
&\times H_{en}(\alpha_e, \beta_d, b_3, b_2, b_1) \phi_D^p(x_3) \left\{ \phi_{B^*}^v(x_1) \phi_D^p(x_2) m_2 m_3 (x_3 - x_2) \right. \\
&\quad \left. + \phi_{B^*}^t(x_1) \phi_D^a(x_2) m_1 m_3 (x_1 - x_3) \right\}, \tag{A8}
\end{aligned}$$

$$\begin{aligned}
\mathcal{A}_e^{LL} &= \mathcal{A}_e^{LR} = \int_0^1 dx_2 \int_0^1 dx_3 \int_0^\infty b_2 db_2 \int_0^\infty b_3 db_3 H_{af}(\alpha_q, \beta_e, b_2, b_3) \\
&\times \alpha_s(t_e) E_{af}(t_e) \left\{ \phi_D^p(x_3) 2 m_3 \left[\phi_D^a(x_2) m_c + \phi_D^p(x_2) m_2 \bar{x}_2 \right] \right. \\
&\quad \left. - \phi_D^a(x_3) \left[\phi_D^a(x_2) (m_1^2 x_2 + m_3^2 \bar{x}_2) + \phi_D^p(x_2) m_2 m_c \right] \right\}, \tag{A9}
\end{aligned}$$

$$\begin{aligned}
\mathcal{A}_f^{LL} &= \mathcal{A}_f^{LR} = \int_0^1 dx_2 \int_0^1 dx_3 \int_0^\infty b_2 db_2 \int_0^\infty b_3 db_3 H_{af}(\alpha_q, \beta_f, b_3, b_2) \\
&\times \alpha_s(t_f) E_{af}(t_f) \left\{ \phi_D^p(x_2) 2 m_2 \left[\phi_D^a(x_3) m_c + \phi_D^p(x_3) m_3 \bar{x}_3 \right] \right. \\
&\quad \left. - \phi_D^a(x_2) \left[\phi_D^a(x_3) (m_1^2 x_3 + m_2^2 \bar{x}_3) + \phi_D^p(x_3) m_3 m_c \right] \right\}, \tag{A10}
\end{aligned}$$

$$\begin{aligned}
\mathcal{A}_g^{LL} &= \frac{1}{N_c} \int_0^1 dx_1 \int_0^1 dx_2 \int_0^1 dx_3 \int_0^\infty b_1 db_1 \int_0^\infty b_2 db_2 \int_0^\infty db_3 H_{an}(\alpha_q, \beta_g, b_1, b_2, b_3) \\
&\times E_n(t_g) \alpha_s(t_g) \left\{ \phi_D^a(x_2) \phi_D^a(x_3) \left[\phi_{B^*}^v(x_1) (s x_2 + 2 m_3^2 x_3 - u \bar{x}_1) \right. \right. \\
&\quad \left. \left. + \phi_{B^*}^t(x_1) m_1 m_b \right] + \phi_{B^*}^v(x_1) \phi_D^p(x_2) \phi_D^p(x_3) m_2 m_3 (x_2 - x_3) \right\}, \tag{A11}
\end{aligned}$$

$$\begin{aligned}
\mathcal{A}_g^{LR} &= \frac{1}{N_c} \int_0^1 dx_1 \int_0^1 dx_2 \int_0^1 dx_3 \int_0^\infty b_1 db_1 \int_0^\infty b_2 db_2 \int_0^\infty db_3 H_{an}(\alpha_q, \beta_g, b_1, b_2, b_3) \\
&\times E_n(t_g) \alpha_s(t_g) \left\{ \phi_D^a(x_2) \phi_D^a(x_3) \left[\phi_{B^*}^v(x_1) (t \bar{x}_1 - 2 m_2^2 x_2 - s x_3) \right. \right. \\
&\quad \left. \left. - \phi_{B^*}^t(x_1) m_1 m_b \right] + \phi_{B^*}^v(x_1) \phi_D^p(x_2) \phi_D^p(x_3) m_2 m_3 (x_2 - x_3) \right\}, \tag{A12}
\end{aligned}$$

$$\begin{aligned}
\mathcal{A}_h^{LL} &= \frac{1}{N_c} \int_0^1 dx_1 \int_0^1 dx_2 \int_0^1 dx_3 \int_0^\infty b_1 db_1 \int_0^\infty b_2 db_2 \int_0^\infty db_3 E_n(t_h) \\
&\times \alpha_s(t_h) \phi_{B^*}^v(x_1) \left\{ \phi_D^a(x_2) \phi_D^a(x_3) (2 m_2^2 x_2 + s x_3 - t x_1) \right. \\
&\quad \left. + \phi_D^p(x_2) \phi_D^p(x_3) m_2 m_3 (x_3 - x_2) \right\} H_{an}(\alpha_q, \beta_h, b_1, b_2, b_3), \tag{A13}
\end{aligned}$$

$$\begin{aligned}
\mathcal{A}_h^{LR} &= \frac{1}{N_c} \int_0^1 dx_1 \int_0^1 dx_2 \int_0^1 dx_3 \int_0^\infty b_1 db_1 \int_0^\infty b_2 db_2 \int_0^\infty db_3 E_n(t_h) \\
&\times \alpha_s(t_h) \phi_{B^*}^v(x_1) \left\{ \phi_D^a(x_2) \phi_D^a(x_3) (u x_1 - s x_2 - 2 m_3^2 x_3) \right. \\
&\left. + \phi_D^p(x_2) \phi_D^p(x_3) m_2 m_3 (x_3 - x_2) \right\} H_{an}(\alpha_q, \beta_h, b_1, b_2, b_3), \tag{A14}
\end{aligned}$$

$$\begin{aligned}
\mathcal{A}_i^{LL} = \mathcal{A}_i^{LR} &= \int_0^1 dx_2 \int_0^1 dx_3 \int_0^\infty b_2 db_2 \int_0^\infty b_3 db_3 \alpha_s(t_i) H_{af}(\alpha_c, \beta_i, b_2, b_3) \\
&\times E_{af}(t_i) \left\{ \phi_D^a(x_2) \phi_D^a(x_3) (m_1^2 \bar{x}_2 + m_3^2 x_2) - \phi_D^p(x_2) \phi_D^p(x_3) 2 m_2 m_3 x_2 \right\}, \tag{A15}
\end{aligned}$$

$$\begin{aligned}
\mathcal{A}_j^{LL} = \mathcal{A}_j^{LR} &= \int_0^1 dx_2 \int_0^1 dx_3 \int_0^\infty b_2 db_2 \int_0^\infty b_3 db_3 \alpha_s(t_j) H_{af}(\alpha_c, \beta_j, b_3, b_2) \\
&\times E_{af}(t_j) \left\{ \phi_D^a(x_2) \phi_D^a(x_3) (m_1^2 \bar{x}_3 + m_2^2 x_3) - \phi_D^p(x_2) \phi_D^p(x_3) 2 m_2 m_3 x_3 \right\}, \tag{A16}
\end{aligned}$$

$$\begin{aligned}
\mathcal{A}_k^{LL} &= \frac{1}{N_c} \int_0^1 dx_1 \int_0^1 dx_2 \int_0^1 dx_3 \int_0^\infty b_1 db_1 \int_0^\infty b_2 db_2 \int_0^\infty db_3 H_{an}(\alpha_c, \beta_k, b_1, b_2, b_3) \\
&\times E_n(t_k) \alpha_s(t_k) \left\{ \phi_D^a(x_2) \phi_D^a(x_3) \left[\phi_{B^*}^v(x_1) (2 m_2^2 x_2 + s x_3 - t x_1) \right. \right. \\
&\left. \left. - \phi_{B^*}^t(x_1) m_1 m_b \right] + \phi_{B^*}^v(x_1) \phi_D^p(x_2) \phi_D^p(x_3) m_2 m_3 (x_3 - x_2) \right\}, \tag{A17}
\end{aligned}$$

$$\begin{aligned}
\mathcal{A}_k^{LR} &= \frac{1}{N_c} \int_0^1 dx_1 \int_0^1 dx_2 \int_0^1 dx_3 \int_0^\infty b_1 db_1 \int_0^\infty b_2 db_2 \int_0^\infty db_3 H_{an}(\alpha_c, \beta_k, b_1, b_2, b_3) \\
&\times E_n(t_k) \alpha_s(t_k) \left\{ \phi_D^a(x_2) \phi_D^a(x_3) \left[\phi_{B^*}^v(x_1) (u x_1 - s x_2 - 2 m_3^2 x_3) \right. \right. \\
&\left. \left. + \phi_{B^*}^t(x_1) m_1 m_b \right] + \phi_{B^*}^v(x_1) \phi_D^p(x_2) \phi_D^p(x_3) m_2 m_3 (x_3 - x_2) \right\}, \tag{A18}
\end{aligned}$$

$$\begin{aligned}
\mathcal{A}_k^{SP} &= \frac{1}{N_c} \int_0^1 dx_1 \int_0^1 dx_2 \int_0^1 dx_3 \int_0^\infty b_1 db_1 \int_0^\infty b_2 db_2 \int_0^\infty db_3 H_{an}(\alpha_c, \beta_k, b_1, b_2, b_3) \\
&\times E_n(t_k) \left\{ \phi_D^a(x_2) \phi_D^p(x_3) m_3 \left[\phi_{B^*}^v(x_1) m_b + \phi_{B^*}^t(x_1) m_1 (x_1 - x_3) \right] \right. \\
&\left. + \phi_D^p(x_2) \phi_D^a(x_3) m_2 \left[\phi_{B^*}^v(x_1) m_b + \phi_{B^*}^t(x_1) m_1 (x_1 - x_2) \right] \right\} \alpha_s(t_k), \tag{A19}
\end{aligned}$$

$$\begin{aligned}
\mathcal{A}_l^{LL} &= \frac{1}{N_c} \int_0^1 dx_1 \int_0^1 dx_2 \int_0^1 dx_3 \int_0^\infty b_1 db_1 \int_0^\infty b_2 db_2 \int_0^\infty db_3 E_n(t_l) \\
&\times \alpha_s(t_l) \phi_{B^*}^v(x_1) \left\{ \phi_D^a(x_2) \phi_D^a(x_3) (u x_1 - s \bar{x}_2 - 2 m_3^2 \bar{x}_3) \right. \\
&\left. + \phi_D^p(x_2) \phi_D^p(x_3) m_2 m_3 (x_2 - x_3) \right\} H_{an}(\alpha_c, \beta_l, b_1, b_2, b_3), \tag{A20}
\end{aligned}$$

$$\begin{aligned}
\mathcal{A}_i^{LR} &= \frac{1}{N_c} \int_0^1 dx_1 \int_0^1 dx_2 \int_0^1 dx_3 \int_0^\infty b_1 db_1 \int_0^\infty b_2 db_2 \int_0^\infty db_3 E_n(t_l) \\
&\times \alpha_s(t_l) \phi_{B^*}^v(x_1) \left\{ \phi_D^a(x_2) \phi_D^a(x_3) (2m_2^2 \bar{x}_2 + s \bar{x}_3 - t x_1) \right. \\
&+ \left. \phi_D^p(x_2) \phi_D^p(x_3) m_2 m_3 (x_2 - x_3) \right\} H_{an}(\alpha_c, \beta_l, b_1, b_2, b_3), \tag{A21}
\end{aligned}$$

$$\begin{aligned}
\mathcal{A}_i^{SP} &= \frac{m_1}{N_c} \int_0^1 dx_1 \int_0^1 dx_2 \int_0^1 dx_3 \int_0^\infty b_1 db_1 \int_0^\infty b_2 db_2 \int_0^\infty db_3 \\
&\times E_n(t_l) \alpha_s(t_l) \phi_{B^*}^t(x_1) \left\{ \phi_D^a(x_2) \phi_D^p(x_3) m_3 (\bar{x}_3 - x_1) \right. \\
&+ \left. \phi_D^p(x_2) \phi_D^a(x_3) m_2 (\bar{x}_2 - x_1) \right\} H_{an}(\alpha_c, \beta_l, b_1, b_2, b_3), \tag{A22}
\end{aligned}$$

where the subscript i of \mathcal{A}_i^j corresponds to the indices of Fig.2; the superscript j refers to three possible Dirac structures $\Gamma_1 \otimes \Gamma_2$ of the operators $(\bar{q}_1 q_2)_{\Gamma_1} (\bar{q}_3 q_4)_{\Gamma_2}$, namely $j = LL$ for $(V - A) \otimes (V - A)$, $j = LR$ for $(V - A) \otimes (V + A)$, and $j = SP$ for $-2(S - P) \otimes (S + P)$.

The function H_i and the Sudakov factor E_i are defined as

$$H_{ef}(\alpha_e, \beta, b_m, b_n) = K_0(b_m \sqrt{-\alpha_e}) \left\{ \theta(b_m - b_n) K_0(b_m \sqrt{-\beta}) I_0(b_n \sqrt{-\beta}) + (b_m \leftrightarrow b_n) \right\}, \tag{A23}$$

$$\begin{aligned}
H_{en}(\alpha_e, \beta, b_3, b_2, b_1) &= \left\{ \theta(-\beta) K_0(b_3 \sqrt{-\beta}) + \frac{\pi}{2} \theta(\beta) \left[i J_0(b_3 \sqrt{\beta}) - Y_0(b_3 \sqrt{\beta}) \right] \right\} \\
&\times \left\{ \theta(b_2 - b_3) K_0(b_2 \sqrt{-\alpha_e}) I_0(b_3 \sqrt{-\alpha_e}) + (b_2 \leftrightarrow b_3) \right\} \delta(b_1 - b_2), \tag{A24}
\end{aligned}$$

$$\begin{aligned}
H_{af}(\alpha, \beta, b_m, b_n) &= \left\{ \theta(b_m - b_n) \left[i J_0(b_m \sqrt{\beta}) - Y_0(b_m \sqrt{\beta}) \right] J_0(b_n \sqrt{\beta}) \right. \\
&+ \left. (b_m \leftrightarrow b_n) \right\} \left\{ i J_0(b_n \sqrt{\alpha}) - Y_0(b_n \sqrt{\alpha}) \right\} \frac{\pi^2}{4}, \tag{A25}
\end{aligned}$$

$$\begin{aligned}
H_{an}(\alpha, \beta, b_1, b_2, b_3) &= \frac{\pi}{2} \left\{ \theta(-\beta) K_0(b_1 \sqrt{-\beta}) + \frac{\pi}{2} \theta(\beta) \left[i J_0(b_1 \sqrt{\beta}) - Y_0(b_1 \sqrt{\beta}) \right] \right\} \\
&\times \left\{ \theta(b_1 - b_2) \left[i J_0(b_1 \sqrt{\alpha}) - Y_0(b_1 \sqrt{\alpha}) \right] J_0(b_2 \sqrt{\alpha}) + (b_1 \leftrightarrow b_2) \right\} \delta(b_2 - b_3), \tag{A26}
\end{aligned}$$

$$E_{ef}(t) = \exp\{-S_{B^*}(t) - S_{\bar{D}}(t)\}, \tag{A27}$$

$$E_{af}(t) = \exp\{-S_{\bar{D}}(t) - S_D(t)\}, \tag{A28}$$

$$E_n(t) = \exp\{-S_{B^*}(t) - S_{\bar{D}}(t) - S_D(t)\}, \tag{A29}$$

$$S_{B^*}(t) = s(x_1, b_1, p_1^+) + 2 \int_{1/b_1}^t \frac{d\mu}{\mu} \gamma_q, \tag{A30}$$

$$S_{\bar{D}}(t) = s(x_2, b_2, p_2^+) + s(\bar{x}_2, b_2, p_2^+) + 2 \int_{1/b_2}^t \frac{d\mu}{\mu} \gamma_q, \quad (\text{A31})$$

$$S_D(t) = s(x_3, b_3, p_3^+) + s(\bar{x}_3, b_3, p_3^+) + 2 \int_{1/b_3}^t \frac{d\mu}{\mu} \gamma_q, \quad (\text{A32})$$

where the subscript $i = ef, en, af, an$ corresponds to the factorizable emission topologies, the nonfactorizable emission topologies, the factorizable annihilation topologies, and the nonfactorizable annihilation topologies, respectively; I_0, J_0, K_0 and Y_0 are Bessel functions; $\gamma_q = -\alpha_s/\pi$ is the quark anomalous dimension; the expression of $s(x, b, Q)$ can be found in of Ref.[14]; α and β are the virtualities of gluon and quarks. the subscript of β_i corresponds to the indices of Fig.2. The definitions of the particle virtuality and typical scale t_i are given as follows.

$$\alpha_e = x_1^2 m_1^2 + x_2^2 m_2^2 - x_1 x_2 t, \quad (\text{A33})$$

$$\alpha_q = x_2^2 m_2^2 + x_3^2 m_3^2 + x_2 x_3 s, \quad (\text{A34})$$

$$\alpha_c = \bar{x}_2^2 m_2^2 + \bar{x}_3^2 m_3^2 + \bar{x}_2 \bar{x}_3 s, \quad (\text{A35})$$

$$\beta_a = m_1^2 + x_2^2 m_2^2 - x_2 t - m_b^2, \quad (\text{A36})$$

$$\beta_b = m_2^2 + x_1^2 m_1^2 - x_1 t - m_c^2, \quad (\text{A37})$$

$$\beta_c = \alpha_e + \bar{x}_3^2 m_3^2 - x_1 \bar{x}_3 u + x_2 \bar{x}_3 s - m_c^2, \quad (\text{A38})$$

$$\beta_d = \alpha_e + x_3^2 m_3^2 - x_1 x_3 u + x_2 x_3 s, \quad (\text{A39})$$

$$\beta_e = m_3^2 + x_2^2 m_2^2 + x_2 s - m_c^2 > 0, \quad (\text{A40})$$

$$\beta_f = m_2^2 + x_3^2 m_3^2 + x_3 s - m_c^2 > 0, \quad (\text{A41})$$

$$\beta_g = \alpha_q + \bar{x}_1^2 m_1^2 - \bar{x}_1 x_2 t - \bar{x}_1 x_3 u - m_b^2, \quad (\text{A42})$$

$$\beta_h = \alpha_q + x_1^2 m_1^2 - x_1 x_2 t - x_1 x_3 u, \quad (\text{A43})$$

$$\beta_i = m_3^2 + \bar{x}_2^2 m_2^2 + \bar{x}_2 s > 0, \quad (\text{A44})$$

$$\beta_j = m_2^2 + \bar{x}_3^2 m_3^2 + \bar{x}_3 s > 0, \quad (\text{A45})$$

$$\beta_k = \alpha_c + \bar{x}_1^2 m_1^2 - \bar{x}_1 \bar{x}_2 t - \bar{x}_1 \bar{x}_3 u - m_b^2, \quad (\text{A46})$$

$$\beta_l = \alpha_c + x_1^2 m_1^2 - x_1 \bar{x}_2 t - x_1 \bar{x}_3 u, \quad (\text{A47})$$

$$t_{a,b} = \max\{\sqrt{-\alpha_e}, \sqrt{|\beta_{a,b}|}, 1/b_1, 1/b_2\}, \quad (\text{A48})$$

$$t_{c,d} = \max\{\sqrt{-\alpha_e}, \sqrt{|\beta_{c,d}|}, 1/b_2, 1/b_3\}, \quad (\text{A49})$$

$$t_{e,f} = \max\{\sqrt{\alpha_q}, \sqrt{|\beta_{e,f}|}, 1/b_2, 1/b_3\}, \quad (\text{A50})$$

$$t_{g,h} = \max\{\sqrt{\alpha_q}, \sqrt{|\beta_{g,h}|}, 1/b_1, 1/b_2\}, \quad (\text{A51})$$

$$t_{i,j} = \max\{\sqrt{\alpha_c}, \sqrt{|\beta_{i,j}|}, 1/b_2, 1/b_3\}, \quad (\text{A52})$$

$$t_{k,l} = \max\{\sqrt{\alpha_c}, \sqrt{|\beta_{k,l}|}, 1/b_1, 1/b_2\}. \quad (\text{A53})$$

- [1] C. Patrignani *et al.* (Particle Data Group), Chin. Phys. C 40, 100001 (2016).
- [2] B. Grinstein, J. Camalich, Phys. Rev. Lett. 116, 141801 (2016).
- [3] G. Xu *et al.*, Eur. Phys. J. C 76, 583 (2016).
- [4] Q. Chang *et al.*, Int. J. Mod. Phys. A 30, 1550162 (2015).
- [5] Q. Chang *et al.*, Adv. in High Energy Phys. 2015, 767523 (2015).
- [6] Q. Chang *et al.*, Eur. Phys. J. C 76, 523 (2016).
- [7] Q. Chang *et al.*, Nucl. Phys. B 909, 921 (2016).
- [8] M. Wirbel, B. Stech, M. Bauer, Z. Phys. C 29, 637 (1985).
- [9] M. Beneke *et al.*, Phys. Rev. Lett. 83, 1914 (1999).
- [10] M. Beneke *et al.*, Nucl. Phys. B 591, 313 (2000).
- [11] M. Beneke *et al.*, Nucl. Phys. B 606, 245 (2001).
- [12] D. Du, D. Yang, G. Zhu, Phys. Lett. B 509, 263 (2001).
- [13] D. Du, D. Yang, G. Zhu, Phys. Rev. D 64, 014036 (2001).
- [14] H. Li, Phys. Rev. D 52, 3958 (1995).
- [15] C. Chang, H. Li, Phys. Rev. D 55, 5577 (1997).
- [16] T. Yeh, H. Li, Phys. Rev. D 56, 1615 (1997).
- [17] G. Buchalla, A. Buras, M. Lautenbacher, Rev. Mod. Phys. 68, 1125, (1996).
- [18] D. Fakirov, B. Stech, Nucl. Phys. B 133, 315 (1978).
- [19] M. Bauer, B. Stech, M. Wirbel, Z. Phys. C 34, 103 (1987).
- [20] G. Lepage, S. Brodsky, Phys. Rev. D 22, 2157 (1980).
- [21] C. Bauer *et al.*, Phys. Rev. D 63, 114020 (2001).

- [22] C. Bauer, D. Pirjol, I. Stewart, Phys. Rev. D 65, 054022 (2002).
- [23] C. Bauer *et al.*, Phys. Rev. D 66, 014017 (2002).
- [24] M. Beneke *et al.*, Nucl. Phys. B 643, 431 (2002).
- [25] P. Ball, V. Braun, Y. Koike, K. Tanaka, Nucl. Phys. B 529, 323 (1998).
- [26] T. Kurimoto, H. Li, A. Sanda, Phys. Rev. D 65, 014007 (2001).
- [27] J. Sun *et al.*, Phys. Lett. B 752, 322 (2016).
- [28] Y. Yang *et al.*, Int. J. Mod. Phys. A 31, 1650146 (2016).
- [29] R. Li, C. Lü, H. Zou, Phys. Rev. D 78, 014018 (2008).
- [30] R. Li *et al.*, Phys. Rev. D 81, 034006 (2010).
- [31] H. Zou *et al.*, J. Phys. G 37, 015002 (2010).
- [32] Y. Li, C. Lü, Z. Xiao, J. Phys. G 31, 273 (2005).
- [33] B. Colquhoun *et al.* (HPQCD Collaboration), Phys. Rev. D 91, 114509 (2015).
- [34] A. Kamal, Particle Physics, Springer, 2014, p. 297, p. 298.
- [35] C. Cheung, C. Hwang, JHEP, 1404, 177 (2014).
- [36] V. Šimonis, Eur Phys J A 52, 90 (2016).
- [37] Ed. A. Bevan *et al.*, Eur. Phys. J. C 74, 3026 (2014).
- [38] Y. Amhis *et al.* (Heavy Flavor Averaging Group), arXiv:1412.7515[hep-ex].
- [39] A. Akeroyd *et al.*, arXiv:1002.5012[hep-ex].
- [40] T. Gershon, M. Needham, Comptes Rendus Physique 16, 435 (2015).